

## SPRINGBACK, INTERNAL ELASTIC ENERGY AND STORED ENERGY

Vratislav Kafka\*

*Author's general mesomechanical concept is applied to explanation of the physical background of the phenomenon of springback and to its modeling. The internal elastic stress field in the material is modeled on the mesoscale and the variations of this field clarify the main features of springback that are observed experimentally in the process of loading, unloading and loading-free creep. Attention is not paid to minute description of the stress-strain diagram appearing in the course of unloading, but to the value of the residual strain after unloading, which is important from the technical point of view. It is shown how creep after unloading depends on stored energy.*

Keywords: *springback, microstructures, constitutive behavior*

### 1. Introduction

Springback is a technically important as well as scientifically interesting phenomenon. Therefore, it had a great attention in the last decades ([1]–[12]). There are two main scientific lines related to this topic: that dealing with geometry of sheet forming and that dealing with material properties. The current study is aimed at the material properties modeled on the basis of the general author's mesomechanical concept [13]. In this concept, the material under study is described as a two-phase continuum with different mechanical properties (one compliant, the other one resistant) as well as different geometry of substructures of the two phases. In this approach, the pivotal point is a special way of description of the geometry of the two substructures by 'structural parameters' (derived as integral forms in distribution functions), whose values can be positive, vanishing or infinite. Their different combinations lead to models of all four possible combinations of connectivity of the two substructures: (i) both substructures continuous, (ii) both substructures discontinuous, (iii) substructure [A] forming inclusions in the matrix of substructure [B], (iv) substructure [B] forming inclusions in the matrix of substructure [A].

As to the material properties of the materials showing springback, one of the essential problems is modeling the behavior of the material in the course of unloading after plastic deformation. The simplest description is linear unloading with the stiffness equal to Young's modulus. However, experimental findings do not corroborate this simple assumption if strain overpasses some limit. A closer description has been proposed: decrease of the elastic stiffness with accumulation of plastic strain [4]. But even this description is not accurate enough, and the next step in approaching the experimental findings was description of unloading by a non-linear curve [9]. This leads to the question: what is the physical background of this decrease of elastic stiffness and of the non-linearity?

---

\* Ing. V. Kafka, DrSc., Institute of Theoretical and Applied Mechanics ASCR, Prosecká 76, 190 00 Prague 9

A qualitative explanation can be seen in the variation of the dislocation structure (e.g. [8]), but receiving quantitative description based on this concept is difficult. Another explanation based on the damage theory has been proposed in [14]. But damage would cause change of elastic stiffness even at the beginning of unloading, which is not observed [9]. At the beginning of unloading, the elastic stiffness equals the initial Young's modulus; only with proceeding unloading the slope of the unloading curve decreases. Apart from these elastic-plastic features, in some materials also the phenomenon of creep plays an important role ([11], [15]).

In what follows, the observed behavior is explained and described by our mesomechanical model.

## 2. Basic relations

The basic notion of our model is representation of a metallic material as a macroscopically homogeneous, but mesoscopically heterogeneous medium with two substructures. The physical nature of one of these substructures corresponds to inner parts of grains that are relatively compliant (superscript c). The physical nature of the other substructure can be different in different materials (precipitates, inclusions, impurities, boundary regions of grains), but for formulation and use of our model, the only important assumption is that such substructure exists, that it is relatively resistant, and that can be modeled as elastic (superscript e). Of course, that such model means simplification of reality, but a number of papers of the author and of his collaborators proved that it leads to a good description of many features of mechanical behavior of many materials. For the use of this concept, it is not necessary to go up to the microscale and to disclose the physical nature and the details of the atomic structure. The model parameters are determinable from macroscopic tests. In our works, this *mesoscale* model has successfully been applied to metallic materials, concrete, polymers and biological tissues ([16], [17], [13], [18], [19]).

Our approach [13] is described by tensorial internal variables. The essential feature of this concept is description of the internal stress fields by taking into account not only the average stresses in the material constituents (substructures), but also the space-dependent fluctuations of the stress fields. This represents an alternative to the concept that works with stress fields around individual dislocations and with piling up of dislocations at the grain boundaries

Here, we are going to use a simple variant of our model that assumes homogeneity of elastic properties and heterogeneity of inelastic properties in the two substructures:

$$v^e \sigma_{ij}^e + v^c \sigma_{ij}^c = \bar{\sigma}_{ij} , \quad (1)$$

$$v^e \varepsilon_{ij}^e + v^c \varepsilon_{ij}^c = \bar{\varepsilon}_{ij} , \quad (2)$$

$$\dot{\varepsilon}_{ij}^e = \mu \dot{s}_{ij}^e , \quad \varepsilon^e = \rho \sigma^e = \rho \bar{\sigma} = \bar{\varepsilon} , \quad (3)$$

$$\dot{\varepsilon}_{ij}^{\prime e} = \dot{\varepsilon}_{ij}^e - \dot{\bar{\varepsilon}}_{ij} , \quad \varepsilon^{\prime e} = \varepsilon^e - \bar{\varepsilon} , \quad (4)$$

$$\dot{\varepsilon}_{ij}^{\prime e} = \mu \dot{s}_{ij}^{\prime e} , \quad \varepsilon^{\prime e} = 0 , \quad (5)$$

$$\dot{\varepsilon}_{ij}^c = \mu \dot{s}_{ij}^c + s_{ij}^c \dot{h}^c , \quad \varepsilon^c = \rho \sigma^c = \rho \bar{\sigma} = \bar{\varepsilon} , \quad (6)$$

$$\dot{\varepsilon}_{ij}^{\prime c} = \dot{\varepsilon}_{ij}^c - \dot{\bar{\varepsilon}}_{ij} , \quad \varepsilon^{\prime c} = \varepsilon^c - \bar{\varepsilon} , \quad (7)$$

$$\dot{\varepsilon}_{ij}^{\prime c} = \mu \dot{s}_{ij}^{\prime c} + s_{ij}^{\prime c} \dot{h}^c , \quad \varepsilon^{\prime c} = 0 , \quad (8)$$

$$s_{ij}^e - s_{ij}^c + \frac{s_{ij}^{\prime e}}{\eta^e} - \frac{s_{ij}^{\prime c}}{\eta^c} = 0 . \quad (9)$$

The meaning of the symbols is given in ‘Nomenclature’. For determination of the 9 tensorial variables  $\sigma_{ij}^e$ ,  $\sigma_{ij}^c$ ,  $\sigma_{ij}^{\prime e}$ ,  $\sigma_{ij}^{\prime c}$ ,  $\varepsilon_{ij}^e$ ,  $\varepsilon_{ij}^c$ ,  $\varepsilon_{ij}^{\prime e}$ ,  $\varepsilon_{ij}^{\prime c}$ ,  $\bar{\varepsilon}_{ij}$  there are 9 tensorial equations (1) to (9) available (if the evolution of  $\bar{\sigma}_{ij}$  is prescribed).

Equations (1), (2), (3) and (6) do not need explanation, equations (4) and (7) define the rates of variables  $e_{ij}^e$  and  $e_{ij}^c$ . The symbols  $\eta^e$ ,  $\eta^c$  characterize the internal structure and are called ‘structural parameters’. Equations (5), (8) and (9) have been derived in the author’s monograph [13]. Their derivation is not simple enough to include it in this short communication.

The integral forms, by which the structural parameters  $\eta^e$ ,  $\eta^c$  have been defined in their deduction, imply that they are non-negative and the higher the value of  $\eta^e$ , the lower is the connectivity of the e-substructure (and analogously for the c-substructure). For an infinite value of  $\eta^e$ , the e-substructure forms discontinuous inclusions. This is an important feature of our model that the *degree of connectivity* of individual substructures can easily be described by the structural parameters.

The internal elastic energy in a macroscopic unit volume of the material is given in terms of internal stresses by the following expression:

$$W^E = \frac{1}{2} \left\{ \mu \left[ v^e \left( s_{ij}^e s_{ij}^e + \frac{1}{\eta^e} s_{ij}^{\prime e} s_{ij}^{\prime e} \right) + v^c \left( s_{ij}^c s_{ij}^c + \frac{1}{\eta^c} s_{ij}^{\prime c} s_{ij}^{\prime c} \right) \right] + 3 \rho \bar{\sigma}^2 \right\} . \quad (10)$$

The meaning of the symbol  $h^c$  differs for elastic deformation from that of elastic-plastic deformation and that of time-dependent deformation.

In the case of elastic deformation

$$\dot{h}^c = 0 . \quad (11)$$

In the case of plastic deformation

$$\dot{h}^c = \frac{d\lambda^c}{dt} , \quad (12)$$

where  $d\lambda^c$  means a scalar measure of the increment of plastic deformation in the c-substructure.

In the case of viscous deformation

$$\dot{h}^c = \frac{1}{2 H^c} , \quad (13)$$

where  $H^c$  means the coefficient of viscosity of the c-substructure.

Starting from this approach, the behavior of the material in the process of springback can be modeled. With the use of equations (1)–(9), the differential form of the mesomechanical constitutive equation can be derived from equations (1)–(9) in a straightforward way [13] to give:

$$d\bar{\varepsilon}_{ij} = d\bar{e}_{ij} + \delta_{ij} d\bar{\varepsilon} = \mu d\bar{s}_{ij} + v^c s_{ij}^c dh^c + \delta_{ij} \rho d\bar{\sigma} , \quad (14)$$

$$ds_{ij}^c = d\bar{s}_{ij} - \frac{v^e}{\mu q} (p s_{ij}^c - \eta^e s_{ij}^{\prime c}) dh^c , \quad (15)$$

$$ds_{ij}^e = d\bar{s}_{ij} + \frac{v^c}{\mu q} (p s_{ij}^c - \eta^e s_{ij}^{\prime c}) dh^c , \quad (16)$$

$$ds'_{ij}{}^c = \frac{\eta^c}{\mu q} [v^e \eta^e s'_{ij}{}^c - (v^c + \eta^e) s'_{ij}{}^c] dh^c, \quad (17)$$

$$ds'_{ij}{}^e = \frac{v^c \eta^e}{\mu q} [\eta^c s'_{ij}{}^c + s'_{ij}{}^c] dh^c, \quad (18)$$

where

$$p = v^e \eta^e + v^c \eta^c, \quad q = p + \eta^e \eta^c. \quad (19)$$

The newly introduced expressions  $p$  and  $q$  have no special physical meaning, their use only simplifies the form of the equations.

The terms  $s'_{ij}{}^e$ ,  $s'_{ij}{}^c$ ,  $s'_{ij}{}^e$ ,  $s'_{ij}{}^c$  represent tensorial internal variables. They are not independent, as  $s'_{ij}{}^e$  and  $s'_{ij}{}^c$  are bound by Eq.(1),  $s'_{ij}{}^e$  and  $s'_{ij}{}^c$  by Eq.(9). Hence, it is possible to reduce the above set of five equations to only three equations, which is used in what follows.

In the case of plastic deformation,  $d\lambda^c$  is to be determined with the use of a yield criterion. In previous author's papers, it has been shown that for metals, the best agreement with experiments gave the following form of the yield criterion:

$$s'_{ij}{}^c s'_{ij}{}^c \leq \frac{3}{2}(c^c)^2 + \frac{1}{\eta^c} s'_{ij}{}^c s'_{ij}{}^c. \quad (20)$$

This is a generalized Mises' criterion, where the second addend on the right-hand side represents the effect of stress-fluctuations. With the use of this criterion, the values of  $d\lambda^c$  can be calculated for very small finite steps that replace the infinitesimal steps in numerical calculations. With the use of the above-presented set of equations (15)–(18) and (20), the differential  $d\lambda^c$  can be expressed as follows:

$$d\lambda^c = 0 \quad \text{for} \quad s'_{ij}{}^c s'_{ij}{}^c < \frac{3}{2}(c^c)^2 + \frac{1}{\eta^c} s'_{ij}{}^c s'_{ij}{}^c, \quad (21)$$

$$d\lambda^c = \frac{d\Lambda^c + |d\Lambda^c|}{2} \quad \text{for} \quad s'_{ij}{}^c s'_{ij}{}^c = \frac{3}{2}(c^c)^2 + \frac{1}{\eta^c} s'_{ij}{}^c s'_{ij}{}^c. \quad (22)$$

where

$$d\Lambda^c = \mu \frac{q s'_{ij}{}^c d\bar{s}_{ij}}{v^e p s'_{ij}{}^c s'_{ij}{}^c - (v^c + \eta^e) s'_{ij}{}^c s'_{ij}{}^c}. \quad (23)$$

### 3. Uniaxial loading and unloading

For uniaxial loading, a new variable  $W$  is defined that corresponds to the energy spent for the deformation process:

$$W = \int_0^{\bar{\varepsilon}_{11}} \bar{\sigma}_{11} d\bar{\varepsilon}_{11}. \quad (24)$$

#### 3.1. Elastic phase of loading

At the beginning of loading, the process is usually elastic, meaning  $dh^c = 0$ . According to criterion (20), this elastic phase ends when  $s'_{11}{}^c$  reaches the value  $c^c$ . Both substructures

are assumed to deform in the same elastic way and this segment of the stress-strain diagram is linear. In Fig. 1, this corresponds to the segment 0-A. In this deformation phase

$$\sigma_{11}^e = \sigma_{11}^c = \bar{\sigma}_{11}, \quad \varepsilon_{11}^e = \varepsilon_{11}^c = \bar{\varepsilon}_{11}, \quad \sigma'_{ij}{}^c = \sigma'_{ij}{}^e = 0, \quad \varepsilon'_{ij}{}^c = \varepsilon'_{ij}{}^e = 0. \quad (25)$$

It is easy to show that in this loading phase  $W = W^E$ :

$$W^E = \frac{1}{2} \left\{ \mu \frac{3}{2} \bar{s}_{11}^2 + 3 \rho \bar{\sigma}^2 \right\} = \frac{\bar{\sigma}_{11}^2}{2E} = \frac{1}{2} E \bar{\varepsilon}_{11}^2 = \int_0^{\bar{\varepsilon}_{11}} \bar{\sigma}_{11} d\bar{\varepsilon}_{11} = W. \quad (26)$$

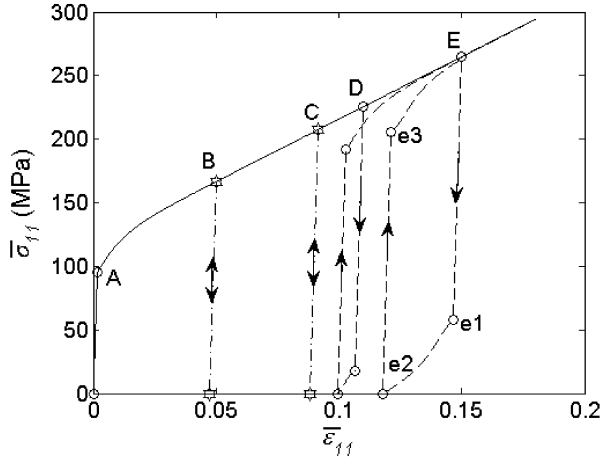


Fig.1: The phenomena of springback for a sample in uniaxial tension at different extents of strain – with the use of true stress

### 3.2. Elastic-plastic phase of loading

After reaching the limit given by criterion (20), an elastic-plastic process starts, in which differential changes of variables follow from equations (14) to (18) to give:

$$d\bar{\varepsilon}_{11} = d\bar{\varepsilon}_{11} + d\bar{\varepsilon} = \mu d\bar{s}_{11} + v^c s_{11}^c dh^c + \rho d\bar{\sigma}, \quad (27)$$

$$ds_{11}^c = d\bar{s}_{11} - v^e \frac{p s_{11}^c - \eta^e s_{11}^c}{\mu q} dh^c, \quad (28)$$

$$ds_{11}^c = \eta^c \frac{v^e \eta^e s_{11}^c - (v^c + \eta^e) s_{11}^c}{\mu q} dh^c \quad (29)$$

with  $dh^c = d\lambda^c$ , and  $d\lambda^c$  given by equations (22) and (23).

In this elastic-plastic deformation phase, the value of  $W$  is higher than that of  $W^E$ , as a part of  $W$  is dissipated, transformed into heat. Under the usually accepted assumption that the process is approximately isothermal, this part is spread out to surroundings. The rest that is not dissipated creates the internal energy  $W^E$ .

In Fig. 1, the elastic-plastic loading phase corresponds to the segment A-B-C-D-E.

With the use of our model equations, the stress-strain diagram can be plotted step-by-step, choosing very small increments of  $\bar{\sigma}_{11}$  and calculating the respective increments of  $\bar{\varepsilon}_{11}$  and of other variables, treating them as differentials.

### 3.3. Elastic-plastic phase of unloading

In the Introduction, the different ways of describing the unloading phase by different authors were shortly outlined. The main features of the unloading lines that are safely found out by experimental observations are:

- (i) At the beginning of the unloading, the elastic stiffness equals the initial Young's modulus.
- (ii) At the end of the unloading line, the residual strain is equal to or smaller than the value that results from purely elastic linear unloading with the initial Young's modulus.
- (iii) At the beginning of reloading that follows unloading, the elastic stiffness equals again the initial Young's modulus.

What is of practical interest, is the final residual strain, not the shape of the unloading stress-strain diagram that depends on the rate of unloading.

According to our model approach, the unloading starts always as linear with the elastic stiffness equal to the initial Young's modulus  $E$ . Up to some limit deformation, the unloading is modeled as linear down to complete unloading. In Fig. 1, this limit is represented by point C. This is the case, in which  $s_{11}^c$  reaches the criterion limit in its negative value, i.e.  $-\sqrt{(c^c)^2 + (s_{11}^c)^2/\eta^c}$  (cf. criterion 20) just for  $\bar{\sigma}_{11} = 0$ . For deformations that reach over C (points D, E in Fig. 1),  $s_{11}^c$  reaches the negative value  $-\sqrt{(c^c)^2 + (s_{11}^c)^2/\eta^c}$  in the course of unloading at  $\bar{\sigma}_{11} > 0$ . With proceeding unloading, the deformation process is elastic-plastic and  $d\bar{\sigma}_{11}/d\bar{\varepsilon}_{11} < E$ . In the framework of our model, this feature is straightforward to explain, as the inelastic part of  $d\bar{\varepsilon}_{11}$  is now nonzero, it has a negative value  $(d\bar{\varepsilon}_{11})_{\text{plast}} = v^c s_{11}^c d\lambda^c$ , where  $d\lambda^c$  is positive by definition and the value of  $s_{11}^c$  is negative (in the course of unloading the value of  $s_{11}^c$  changed from positive value  $\sqrt{(c^c)^2 + (s_{11}^c)^2/\eta^c}$  to negative value  $-\sqrt{(c^c)^2 + (s_{11}^c)^2/\eta^c}$ ). The courses of changes of  $c_{11}^c$  are shown in Fig. 2 in the processes of loading, unloading and reloading for different limits of deformation.

It is clear enough that in the inelastic part of unloading segment  $e_1$ - $e_2$  (Figs. 1-2) some energy must be dissipated. The source of this energy is the internal energy  $W^E$ . In Fig. 3, the drop of  $W^E$  caused by the elastic part of unloading is marked  $\delta W^E$ . Its value is relatively low. However,  $\Delta W^E$  – the drop of  $W^E$  caused by total unloading – elastic plus plastic – is substantially higher.

Thus, the value of  $W^E$  at point C is reduced by  $\Delta W^E$  due to elastic-plastic unloading and the rest represents the so-called stored energy  $SW^E$ . In Fig. 4, the relation between the value of  $SW^E$  in comparison to  $W$  is shown to correspond to the values of  $SW^E$  measured calorimetrically for different materials [20].

It is interesting to analyze the value of  $SW^E$  (value of  $W^E$  at point  $e_2$  corresponding to full unloading) splitting it into two parts:

$$SW^E = (SW^E)^\oplus + (SW^E)^\otimes, \quad (30)$$

where

$$(SW^E)^\oplus = \frac{1}{2} \left\{ \mu \frac{3}{2} [v^e (s_{11}^e)^2 + v^c (s_{11}^c)^2] + 3 \rho \bar{\sigma}^2 \right\}_{e_2} \quad (31)$$

means that part of the stored energy  $SW^E$  that is represented by the average stresses in the

two substructures, whereas

$$(SW^E)^\otimes = \frac{1}{2} \left\{ \mu \frac{3}{2} \left[ \frac{v^e (s_{11}^e)^2}{\eta^e} + \frac{v^c (s_{11}^c)^2}{\eta^c} \right] \right\}_{e_2} \quad (32)$$

means that part of the stored energy  $SW^E$  that is represented by the space-dependent fluctuations.

In many models of composite materials, only the average stresses in the material constituents are taken into consideration. However, in what follows the value of  $(SW^E)^\otimes$  is shown to be substantially higher than  $(SW^E)^\oplus$ . This means that  $(SW^E)^\otimes$  must not be neglected to receive a realistic model.

### 3.4. Creep after unloading

After full unloading from macroscopic stress, the deformation process is usually seen as finished. However, it is not always the case. Thus it was revealed in [15] that the specimen shapes for aluminum alloys can continue to change for long periods following forming and unloading. Steels tested under identical conditions showed no such time-dependent springback.

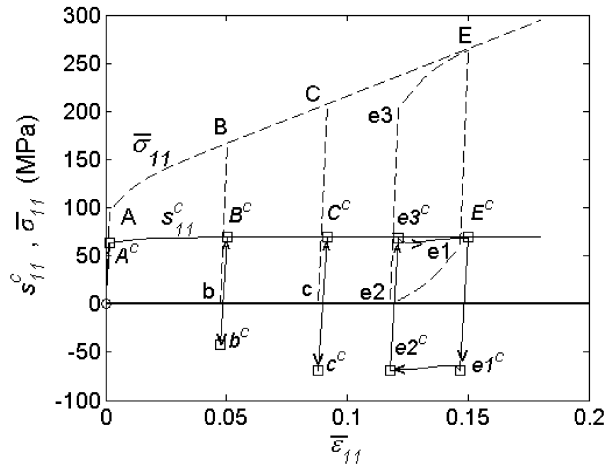


Fig.2: Courses of the main deviatoric stress component  $s_{11}^c$  in the compliant substructure in the deformation processes shown in Fig. 1

From the point of view of our concept, it is easy to explain why such creep can appear. In Fig. 2, the stress component  $s_{11}^c$  is shown to take on the negative value  $-\sqrt{(c^c)^2 + (s_{11}^c)^2}/\eta^c$  after sufficiently large deformation. Without the effect of the e-constituent, this would cause shortening of the specimen, either elastic or viscous. However, it is clear from the preceding considerations that the elastic as well as plastic deformation has stopped and cannot proceed. On the other hand, the time-dependent creep can in some materials proceed according to equations (6) and (13). With proceeding creep, the absolute value of  $s_{11}^c$  diminishes (cf. Eq. (15)) and so does the rate of creep (cf. Eq. (14)).

Two factors decide whether the creep will appear. Firstly, it is temperature [21], as  $H^c$  is temperature dependent. Secondly, the stored energy must be high enough to supply sufficient energy for dissipation in the course of creep. After spending some sufficient part of stored energy for dissipation, the process will stop at some limit  $(W^E)_L$ , from which the value of  $W^E$  is not high enough for the creep to go on.

#### 4. Numerical example

Let us apply our model to an aluminum alloy with the following material parameters:  $\mu = 2.28 \times 10^{-5} \text{ MPa}^{-1}$ ,  $\rho = 5.4 \times 10^{-6} \text{ MPa}^{-1}$ ,  $c^c = 63.66 \text{ MPa}$ ,  $v^e = 0.056$ ,  $v^c = 0.944$ ,  $\eta^e = 2.7433125$ ,  $\eta^c = 0.011429242$ ,  $H^c = 50000 \text{ MPa h}$ .

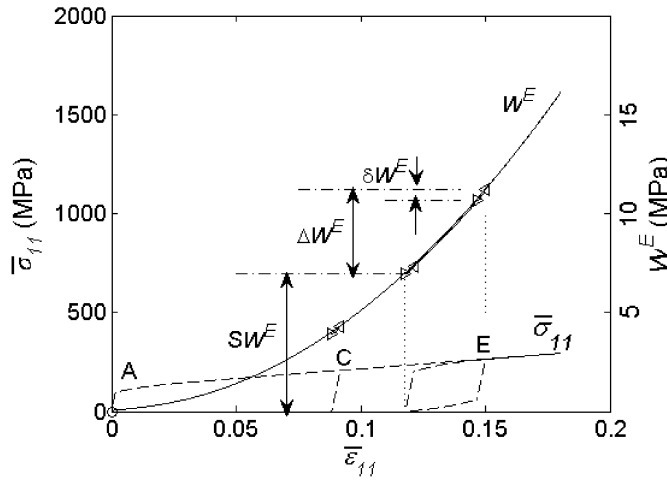


Fig.3: Course of the internal elastic energy  $W^E$  in the processes of loading and unloading shown in Fig. 1

The graphical demonstrations in Figs. 1 to 5 were based on these material parameters. The main general results are presented in the preceding sections. From the numerical results, the values of the two parts of stored energy deserve special attention :

$$(SW^E)^\oplus = 1.351 \text{ MPa} , \quad (SW^E)^\otimes = 5.624 \text{ MPa} , \quad (33)$$

which verifies the importance of taking into account the energy of space-dependent fluctuations.

Another numerical result of interest is the relation of the value of stored energy  $SW^E$  to the energy  $W$  spent for the deformation process from which the value of  $SW^E$  stems. The value of this relation turned out to be :

$$\frac{SW^E}{W} = 0.246 .$$

This means that stored energy for our material and the respective loading strain represents about 25% of the energy spent for realization of the deformation process. This is in the range of results received with the use of calorimetric measurements for different metallic materials [20].

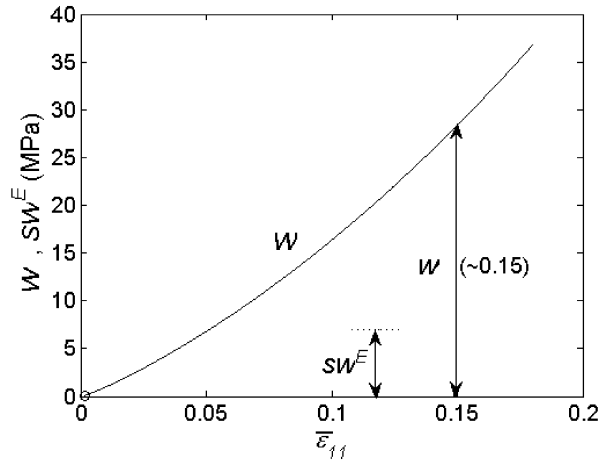


Fig.4: Course of the energy  $W$  spent for deformation of the sample – compared with stored energy  $SW^E$  after 0.15 strain and unloading

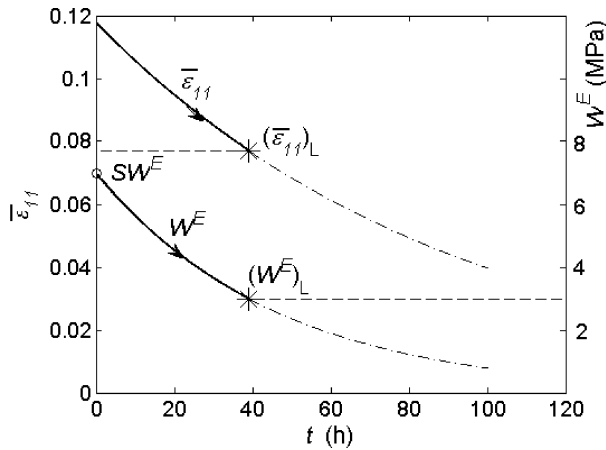


Fig.5: Decrease of the values of internal elastic energy  $W^E$  (starting from the stored energy  $SW^E$ ) and of residual strain due to creep that spends and dissipates stored energy. For values of internal energy under  $(W^E)_L$  the process cannot proceed

**5. Conclusion**

The author’s mesomechanical model applied to the explanation and description of spring-back clarifies the energetic internal processes in the material that lead to springback. Comparison of the main features observed in the course of springback with the outcomes of our model verifies its justness.

**Acknowledgement**

This work has been supported by the Grant Agency of the Czech Republic, Grant GA ČR 103/09/2101.

## Nomenclature

$c^c$	limit value of $s_{11}^c$ at the start of plastic deformation in a uniaxial elastic-plastic process
$\bar{e}_{ij}$ $\{e_{ij}^e, e_{ij}^c\}$	macroscopic {mesoscopic} deviatoric strain
$e_{ij}^e$ $\{e_{ij}^c\}$	deviatoric parts of $\varepsilon_{ij}^e$ $\{\varepsilon_{ij}^c\}$
$E$	Young's modulus
$\dot{h}^c$	formal variable that equals 0 in elasticity, $\dot{\lambda}^c$ in plasticity, and $1/(2H^c)$ in creep
$H^c$	coefficient of viscosity in the c-constituent
$i, j$	indices that can take on the values 1, 2, 3; their repetition means summation
$e \{c\}$	superscripts that relate the respective value to the resistant e-substructure {to the compliant c-substructure}; repetition does not mean summation
$\bar{s}_{ij}$ $\{s_{ij}^e, s_{ij}^c\}$	macroscopic {mesoscopic} deviatoric stress
$s_{ij}^e$ $\{s_{ij}^c\}$	deviatoric parts of $\sigma_{ij}^e$ $\{\sigma_{ij}^c\}$
$t$	time measured in hours
$v^e$	volume fraction of the resistant constituent
$v^c (= 1 - v^e)$	volume fraction of the compliant constituent
$W$	energy spent in the course of the deformation process
$W^E$	elastic energy of internal stresses comprised in a volume unit of the whole material
$SW^E$	stored energy
$(SW^e)^\oplus$	that part of the stored energy $SW^E$ that corresponds to the average stresses in the two substructures
$(SW^e)^\otimes$	that part of the stored energy $SW^E$ that corresponds to the space-dependent fluctuations
$\delta_{ij}$	Kronecker delta
$\bar{\sigma}_{ij}$ $\{\bar{\varepsilon}_{ij}\}$	macroscopic stress {strain}
$\sigma_{ij}^e$ $\{\sigma_{ij}^c\}$	mesoscopic stress in the elastic resistant {inelastic compliant} substructure – averaged values in the respective substructure
$\sigma_{ij}^e$ $\{\sigma_{ij}^c\}$	stresses related to $\varepsilon_{ij}^e$ $\{\varepsilon_{ij}^c\}$ similarly as are $\sigma_{ij}^e$ $\{\sigma_{ij}^c\}$ related to $\varepsilon_{ij}^e$ $\{\varepsilon_{ij}^c\}$
$\delta_{ij}\bar{\sigma}$ $\{\delta_{ij}\sigma^e, \delta_{ij}\sigma^c\}$	macroscopic {mesoscopic} isotropic part of the stress tensors
$\delta_{ij}\sigma^e$ $\{\delta_{ij}\sigma^c\}$	isotropic parts of $\sigma_{ij}^e$ $\{\sigma_{ij}^c\}$
$\varepsilon_{ij}^e$ $\{\varepsilon_{ij}^c\}$	mesoscopic strain in the elastic resistant {inelastic compliant} substructure – averaged values in the respective substructure
$\delta_{ij}\bar{\varepsilon}$ $\{\delta_{ij}\varepsilon^e, \delta_{ij}\varepsilon^c\}$	macroscopic {mesoscopic} isotropic parts of the strain tensor
$\varepsilon_{ij}^e = \varepsilon_{ij}^e - \bar{\varepsilon}_{ij}$ $\{\varepsilon_{ij}^c = \varepsilon_{ij}^c - \bar{\varepsilon}_{ij}\}$	definitions of variables $\varepsilon_{ij}^e$ $\{\varepsilon_{ij}^c\}$
$\delta_{ij}\varepsilon^e$ $\{\delta_{ij}\varepsilon^c\}$	isotropic parts of $\varepsilon_{ij}^e$ $\{\varepsilon_{ij}^c\}$

$\eta^e, \eta^c$	positive ‘structural parameters’ that characterize the structure of the material [ $\eta^e = \eta^c = 0$ corresponds to Voigt’s homogeneous strain model, $\eta^e = \eta^c = \infty$ corresponds to Reuss’ homogeneous stress model, generally higher value {lower value} of one of the parameters describes a lower {higher} connectivity of the respective substructure. In their deduction [13], they have been defined as integral forms in the distribution functions of microscopic stress-fields and strain-fields, but the user of the model works only with these parameters, without specifying the distribution functions themselves]
$\lambda^c$	scalar measure of plastic deformation in the c-constituent
$\Lambda^c$	formal expression whose differential increment $d\Lambda^c$ is defined by Eq. (23); in an active plastic process $d\Lambda^c > 0$ and $d\lambda^c = d\Lambda^c$ , otherwise $d\lambda^c = 0$
$\nu$	Poisson’s ratio
$\mu = (1 + \nu)/E$	deviatoric elastic compliance
$\rho = (1 - 2\nu)/E$	isotropic elastic compliance

## References

- [1] Karafillis A.P., Boyce M.C.: Tooling design in sheet metal forming using springback calculations, *Int. J. Mech. Sci.* 34 (1992) 113–131
- [2] Karafillis A.P., Boyce M.C.: Tooling and binder design for sheet metal forming processes compensating springback error, *Int. J. Mach. Tools Manufact.* 36 (1996) 503–526
- [3] Makinouchi A.: Sheet metal forming simulation in industry, *J. Mater. Proc. Technol.* 60 (1996) 19–26
- [4] Morestin F., Boivin M., Silva C.: Elastoplastic formulation using a kinematic hardening model for springback analysis in sheet metal forming, *J. Mater. Proc. Technol.* 56 (1996) 619–630
- [5] Zhang L.C., Lin Z.: An analytical solution to springback of sheet metal stamped by rigid punch and elastic die, *J. Mater. Proc. Technol.* 63 (1997) 49–54
- [6] Lee S.W., Yang D.Y.: An assessment of numerical parameters influencing springback in explicit finite element analysis of sheet metal forming process, *J. Mater. Proc. Technol.* 80–81 (1998) 60–67
- [7] Asnafi N.: On springback of double-curved autobody panels, *Int. J. Mech. Sci.* 43 (2001) 5–37
- [8] Carden W.D., Geng M., Matlock D.K.: Measurement of springback, *Int. J. Mech. Sci.* 44 (2002) 79–101
- [9] Cleveland R.M., Ghosh A.K.: Inelastic effect on springback in metals, *Int. J. Plasticity* 18 (2002) 769–785
- [10] Smith L.M., Averill R.C., Lucas J.P., Stoughton T.B., Matin T.B.: Influence of transverse normal stress on sheet metal formability, *Int. J. Plasticity* 19 (2003) 1567–1583
- [11] Ho K.C., Lin J., Dean T.A.: Modelling of springback in creep forming thick aluminum sheets, *Int. J. Plasticity* 20 (2004) 733–751
- [12] Eggersten P.A., Mattiasson K.: On constitutive modeling for springback analysis, *Int. J. Mech. Sci.* 52 (2010) 804–818
- [13] Kafka V.: *Mesomechanical Constitutive Modeling*, World Scientific, Singapore 2001
- [14] Thibaud S., Boudeau N., Gelin J.C.: Coupling effects of hardening and damage necking and bursting conditions in sheet metal forming, *Int. J. Damage Mechanics* 13 (2004) 107–122
- [15] Wang J.F., Wagoner R.H., Carden W.D., Matlock D.K., Barlat F.: Creep and anelasticity in the springback of aluminum, *Int. J. Plasticity* 20 (2004) 2209–2232
- [16] Kafka V.: On constitutive equations of quasihomogeneous materials, *Zeitschrift für angewandte Mathematik und Mechanik* 59 (1979) 423–430
- [17] Kafka V.: *Inelastic Mesomechanics*, World Scientific, Singapore 1987

- [18] Kafka V.: Concrete under complex loading: Mesomechanical model of deformation and cumulative damage, *European Journal of Mechanics – A/Solids* 23 (2004) 63–75
- [19] Kafka V.: Shape memory polymers: A mesoscale model of the internal mechanism leading to the SM phenomena, *Int. J. Plasticity* 24 (2008) 1533–1548
- [20] Kafka V.: Strain-hardening and stored energy, *Acta Technica ČSAV* 24 (1979) 199–216
- [21] Greze R., Manach P.Y., Laurent H., Thuillier S., Menezes L.F.: Influence of the temperature on residual stresses and springback effect in an aluminium alloy, *Int. J. Mech. Sci.* 52 (2010) 1094–1100

*Received in editor's office:* February 3, 2012

*Approved for publishing:* June 2, 2012